Conserved behavioral circuits govern high-speed decision-making in wild fish shoals

Andrew M. Hein[a,b,1], Michael A. Gil[a,b,c], Colin R. Twomey[d], Iain D. Couzin[e,f,g], and Simon A. Levin[h,i]

[a]Southwest Fisheries Science Center, National Oceanic and Atmospheric Administration, Santa Cruz, CA 95060; [b]Institute of Marine Sciences, University of California, Santa Cruz, CA 95060; [c]Department of Environmental Science & Policy, University of California, Davis, CA 95616; [d]Department of Biology, University of Pennsylvania, Philadelphia, PA 19104; [e]Department of Biology, University of Konstanz, 78457 Konstanz, Germany; [f]Department of Collective Behaviour, Max Planck Institute for Ornithology, 78464 Konstanz, Germany; [g]Chair of Biodiversity and Collective Behaviour, University of Konstanz, 78457 Konstanz, Germany; [h]Department of Ecology and Evolutionary Biology, Princeton University, Princeton, NJ 08544; and [i]Princeton Environmental Institute, Princeton University, Princeton, NJ 08544

Edited by Raghavendra Gadagkar, Indian Institute of Science, Bangalore, India, and approved October 12, 2018 (received for review May 28, 2018)

To evade their predators, animals must quickly detect potential threats, gauge risk, and mount a response. Putative neural circuits responsible for these tasks have been isolated in laboratory studies. However, it is unclear whether and how these circuits combine to generate the flexible, dynamic sequences of evasion behavior exhibited by wild, freely moving animals. Here, we report that evasion behavior of wild fish on a coral reef is generated through a sequence of well-defined decision rules that convert visual sensory input into behavioral actions. Using an automated system to present visual threat stimuli to fish in situ, we show that individuals initiate escape maneuvers in response to the perceived size and expansion rate of an oncoming threat using a decision rule that matches dynamics of known loom-sensitive neural circuits. After initiating an evasion maneuver, fish adjust their trajectories using a control rule based on visual feedback to steer away from the threat and toward shelter. These decision rules accurately describe evasion behavior of fish from phylogenetically distant families, illustrating the conserved nature of escape decision-making. Our results reveal how the flexible behavioral responses required for survival can emerge from relatively simple, conserved decision-making mechanisms.

predator–prey interactions | neural circuit | neuroethology | decision-making | evasion

Avoiding predators is an essential task for wild animals (1). Because fleeing at the wrong time can be costly (2, 3), theory predicts that animals have evolved mechanisms for initiating escapes when the threat of attack is high, and suppressing them when the threat is low (2, 4). Once an animal decides to flee, the most favorable evasion trajectory depends on the actions of its predator and features of the landscape (3, 5), implying the need for continuous behavioral adjustments in response to sensory feedback (6).

Despite the fact that these tasks can differ considerably from one setting to another, laboratory experiments suggest that a wide range of animal species translate sensory information into evasive actions using strategies that are similar at both the neural and behavioral levels (7). These similarities imply the existence of conserved mechanisms for detecting and responding to predators that govern animal escape decisions in the wild (8). A major challenge in testing this hypothesis, however, has been the difficulty of linking sensory and decision-making mechanisms studied in the laboratory (9–12) to behaviors observed in the field (13). This has proven challenging, in part, due to the difficulty of reconstructing and experimentally manipulating the sensory cues perceived by wild, freely moving animals (14, 15). Consequently, the connection between evasion behaviors of wild animals and the mechanisms that underlie them remains a missing piece in our understanding of animal decision-making (1).

To address this deficit, we studied the predator evasion behavior of wild coral reef fish in Mo'orea, French Polynesia (Fig. 1*A*). These ecologically important species forage in shallow reef flats where they are vulnerable to predators such as reef sharks (16), moray eels (17), and human spearfishers (18). Reef fish forage in loose, mixed-species groups that can vary in size by over an order of magnitude (18). The size of these groups appears to affect evasion decisions of individual fish (18, 19), but the sensory mechanisms that guide these decisions are poorly understood.

Fish could perceive predators and one another using a variety of sensory cues, including pressure changes (20), sounds (21), or olfactory stimuli. Visual cues, in particular, appear to be important in triggering and guiding fish escape behavior (11, 12). Laboratory studies of model fish species, for example, have identified a system of neural circuits in the brain that responds strongly and selectively to looming visual stimuli—expanding images that simulate objects approaching the eye (10, 11, 22). This selectivity for looming objects—also present in amphibians, birds, insects, and humans—has been hypothesized to provide a conserved mechanism for detecting an approaching predator in complex natural scenes (7, 8). Furthermore, some loom-sensitive pathways can integrate the motion of an approaching object with other features in a visual scene (23). These decision-making circuits could, thus, serve to both detect predators (7) and integrate visual information about risk such as the locations of nearby individuals that share common predators (6). However, the degree to which loom-sensitive circuits govern escape decision-making of wild animals is not currently known.

Significance

To survive, animals must quickly detect and respond to predators. However, the rules wild animals use to translate sensory cues into evasion decisions remain largely unknown. We developed an automated system to present visual threat stimuli to mixed-species groups of foraging fish in a coral reef. Using hundreds of stimulus presentations to fish from nine families, we show that escape decisions are governed by a conserved set of decision-making rules that transform sensory input into evasive actions. Our methodology allows us to quantitatively analyze these rules, revealing both how they map onto previously studied neural circuits and how they function under dynamic natural conditions.

Author contributions: A.M.H., M.A.G., C.R.T., I.D.C., and S.A.L. designed research; A.M.H. performed research; A.M.H., M.A.G., and C.R.T. contributed new reagents/analytic tools; A.M.H. and C.R.T. analyzed data; and A.M.H., M.A.G., C.R.T., I.D.C., and S.A.L. wrote the paper.

The authors declare no conflict of interest.

This article is a PNAS Direct Submission.

[1]To whom correspondence should be addressed. Email: ahein@ucsc.edu.

This article contains supporting information online at www.pnas.org/lookup/suppl/doi:10.1073/pnas.1809140115/-/DCSupplemental.

Published online November 12, 2018.

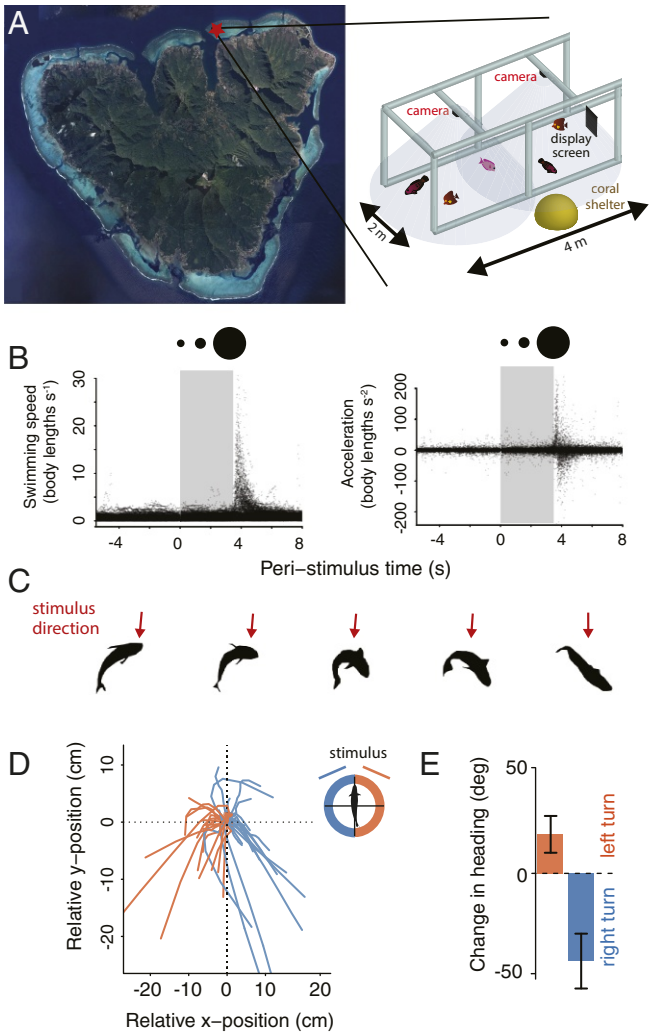

Fig. 1. Looming visual stimuli trigger evasion maneuvers in wild fish. (*A*) Experimental arena deployed in coral reef. Satellite image courtesy of Google Earth, © 2018 Digital Globe and CNES/Airbus. Data courtesy of LDEO-Columbia, NSF, NOAA, SIO, US Navy, NGA, and GEBCO. (*B*) Swimming speeds (*Left*) and accelerations (*Right*) of fish before, during (gray band), and after presentation of loom stimulus. (*C*) Sequence of body postures during response of a parrotfish (*C. sordidus*) before accelerating. The arrows indicate the frame measurements in the horizontal dimensions indicated by "2m" and "4m" in *A, Right*. (*D*) Escape trajectories of fish that viewed stimulus in the right (orange) and left (blue) visual hemisphere (first 150 ms of trajectories shown). (*E*) Mean flight angle (±2 SE) of escape trajectories shown in *D* (LRT using von Mises distribution: $p = 2.10 \times 10^{-5}$).

To investigate these mechanisms, we engineered a high-throughput system to present looming visual threats to coral reef fish in situ. Our experimental system consisted of a camera frame deployed in a reef flat, within which we positioned a tablet computer to display visual stimuli (Fig. 1*A*). The frame was placed alongside a colony of mounding coral (*Porites* sp.), which provided a natural structural refuge for fish (18). At predetermined times, a looming stimulus was displayed on the tablet screen, and fish were recorded by downward-facing video cameras. Fish locations and headings were subsequently tracked using custom computer vision software (see *SI Appendix* for full experimental protocol).

Results

The looming stimulus triggered rapid accelerations and swimming speeds far outside the range observed before stimulus presentation (Fig. 1*B* and Movie S1) in 12 phylogenetically diverse species, including surgeonfish (*Acanthurus nigrofuscus, Ctenochaetus striatus, Zebrasoma scopas*), Moorish idols (*Zanclus cornatus*), parrotfish (*Scarus psittacus, Chlorurus sordidus*), pufferfish (*Arothron meleagris*), butterflyfish (*Chaetodon vagabundus, Forcipiger flavissimus*), wrasses (*Halichoeres hortulanus*), triggerfish (*Rhinecanthus aculeatus*), and goatfish (*Mulloidichthys avolineatus*). Because fish swam freely through the arena, the position of the stimulus in their visual fields was not fixed. However, the initial direction of escape trajectories (Fig. 1*C*) was predictable based on the location of the stimulus in an individual's visual field before its response (Fig. 1*D*). Individuals that perceived the stimulus in the right visual hemisphere turned to the left, and vice versa (Fig. 1*E*). These rapid turns moved the animal's head out of the perceived path of the looming object (4), and are consistent with the prediction that prey should avoid high-speed attacks by turning (3, 5), a strategy known as the turning gambit. This highly polar turning response (Fig. 1*C*) also resembles responses to looming objects reported in laboratory studies of Mauthner cell- and reticulospinal circuit-mediated escape responses of zebrafish (10, 22), potentially implicating these circuits in mediating the behavior of wild fish, as we discuss in more detail in *Initiation of Escape Responses* below.

Initiation of Escape Responses. Not all stimulus presentations triggered escape maneuvers. To determine how the probability of response depended on the sensory cues perceived by each fish, we reconstructed the perceived sizes and locations of the looming stimulus and neighboring fish in the visual field of each fish over the course of the trial (Fig. 2*A* and Movie S2). We used these visual features to construct a model of escape decision-making that predicted probability of response, P: $P = 1/(1 + e^{-D})$, where D is a decision function that describes how a fish integrates the sensory cues available to it (see *SI Appendix* for details and full model formulation).

For animals that forage in groups, the risk posed by an attacking predator depends not only on the predator's speed and initial location but also on the presence and locations of other vulnerable individuals (6). In past work, we found that the propensity of coral reef fish to flee from foraging areas when confronted with threatening stimuli depends on the density of other fish in the area (18). However, we were unable to identify the mechanisms by which fish perceive one another and modify escape decision-making. Motivated by our previous results and the finding that these species respond strongly to visual cues (Fig. 1), we hypothesized that fish decide whether to flee from a looming object by integrating the perceived visual expansion rate of the object (7, 24) with visual information about the presence and locations of nearby individuals [i.e., "neighbors" (6, 12)]. Such a decision rule can be captured by the function $D = \delta + \alpha S' \exp[\sum_i \gamma_i F_i]$, where δ and α are constants, S' is the perceived expansion rate of the looming object (8, 24), F_i represent visual features of the scene (e.g., perceived sizes of neighbors; Fig. 2*A*), and γ_i are parameters that determine how changes in F_i affect the decision to respond. We compared a large set of models containing different combinations of visual features, F_i, to determine how a fish's decision to respond depends on the visual cues it perceives (*SI Appendix*). To ensure that we were modeling fish that responded directly to the stimulus rather than to escape responses of other fish, we restricted this analysis to first responders (first fish to respond in a given trial) and nonresponders (full dataset contained 84 total responders, 47 first responders, and 574 nonresponders). First responder (FR) and nonresponder (NR) counts by family were Acanthuridae (FR = 4, NR = 238), Scaridae (FR = 23, NR = 203), Zanclidae (FR = 13, NR = 43), Labridae (FR = 3, NR = 40), Chaetodontidae (FR = 1, NR = 24), Balistidae (FR = 1, NR = 15), Mullidae (FR = 1, NR = 9), Tetradontidae (FR = 1, NR = 3), and Serranidae (FR = 0, NR = 2). Acanthuridae, Scaridae, and Zanclidae were

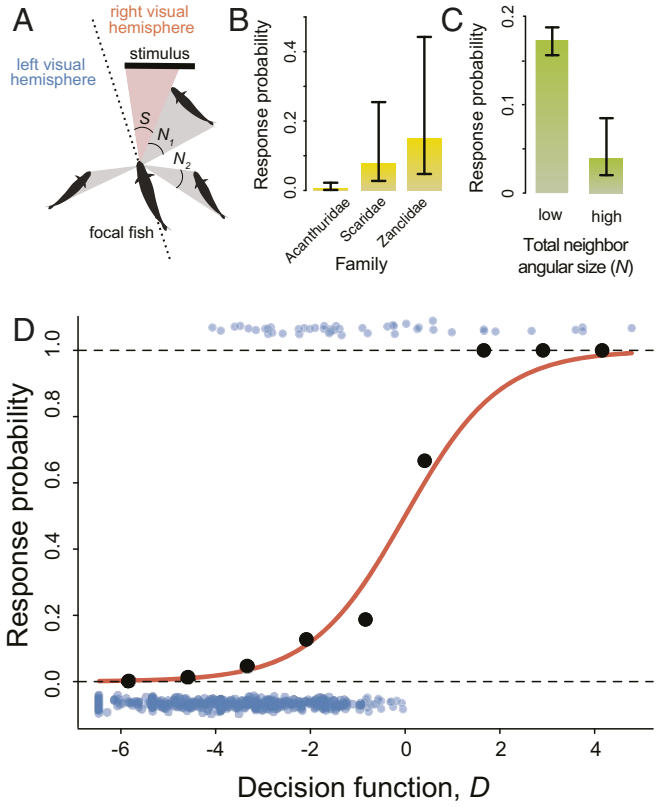

Fig. 2. Fish integrate visual features of stimulus and neighboring fish when deciding whether to flee. (*A*) Method for computing perceived angular size of stimulus and neighboring fish (see *SI Appendix* for details and alternative method): S is perceived angular size of stimulus measured as the angular region of fish's visual field occupied by looming image; $N = N_1 + N_2$ is total angular size of neighbors in visual hemisphere containing stimulus (N_1 and N_2 are angular sizes of neighbors). (*B*) Predicted response probability (and 95% CI) based on Eq. **1** for the three most common fish families, with S, S' and N set to mean of observed values. (*C*) Predicted response probability (and 95% CI) when N is low (25th percentile of observed N values) or high (75th percentile). The δ_j is set to the mean for all families, and S and S' are set to 75th percentile of observed values. (*D*) Observed response data (blue points vertically offset; 1 = response, 0 = no response), empirical response probabilities (black points), and predicted response probability based on Eq. **1** (orange line).

the most common families present. For the purpose of analysis, these three families were separated, and the six rarer families were combined into a single group (see *SI Appendix*).

Our analysis revealed that response probability is best predicted by a function of three visual features (Fig. 2 *B*–*D*): the perceived angular size, S, and expansion rate, S', of the looming image (Fig. 2*A*), and the total perceived angular size, N, of neighbors in the visual hemisphere containing the stimulus (Fig. 2*D*),

$$D = \delta_j + \alpha S' e^{-\beta S} e^{-\gamma N} \qquad \alpha, \beta, \gamma > 0. \qquad [1]$$

Individuals are more likely to initiate escapes when the perceived expansion rate of the looming object, S', is large [Likelihood ratio test (LRT), $p = 4.1 \times 10^{-13}$]; however, the perceived size of the object, S, inhibits responses, such that, when an object appears larger, it must also expand more quickly to elicit the same response (LRT, $p = 1.8 \times 10^{-6}$), a result also reported in laboratory studies (7, 8). The constant, δ_j, captured differences in response threshold among fish in different families (e.g., Acanthuridae, Zanclidae; Fig. 2*B*). Eq. **1** predicted accurately for each family (out-of-sample prediction accuracy 82 to 98%; *SI Appendix*, Fig. S4), suggesting that behavior of phylogenetically diverse species can be explained by a common decision rule, with among-family differences in response threshold that could reflect differences in risk perception (19), visual sensitivity (25), or other factors.

The excitation of responses by object expansion rate and inhibition by object size (i.e., the term $\alpha S' e^{-\beta S}$ in Eq. **1**) revealed by our analysis has precisely the same form as that previously described in laboratory experiments with both vertebrates and invertebrates (7, 8, 24). However, our analysis also revealed a second source of inhibition that has not, to our knowledge, been previously described. In particular, individuals are less likely to initiate escapes when the perceived size of neighbors, N, in the visual hemisphere containing the stimulus is high (Eq. **1**; LRT for effect of N, $p = 7.8 \times 10^{-6}$; Fig. 2*C*). This effect is not due solely to visual occlusion of the stimulus by neighboring individuals, which is accounted for in our calculation of perceived stimulus size and expansion rate (Fig. 2*A* and *SI Appendix*, Fig. S3). Instead, this finding implies that fish scale reactivity up or down depending on the locations of other nearby fish. As a result, an individual is most likely to respond when it is the closest fish to the looming object. This finding supports the hypothesis that the nervous system integrates information about a threat with the perceived locations of other objects before initiating escapes (21). It also provides a sensory mechanism for the well-known "risk dilution" effect (1): the observation that animals in large groups often respond less readily to threat-related stimuli than do animals in small groups (13, 18), a behavior that may be necessary to avoid hypersensitivity when foraging in groups (18).

Alternative models that provide a reasonably good fit to the data share the three primary features of Eq. **1**: excitation by perceived object expansion rate, and inhibition by perceived object size and visual features of neighbors (*SI Appendix*, *Response Probability Analysis* and Table S1). Thus, although Eq. **1** provided the best fit to data, all of the top models lead to the same qualitative inferences about the effects of the features of the looming object and the effect of neighbors on response probability.

Trajectory Control During Evasion Maneuvers. After initiating evasion maneuvers, fish turned sharply away from the stimulus, then appeared to bias their trajectories toward the coral structure to the east of the arena (Figs. 1*A* and 3 *A* and *B*). Many animals control their trajectories during locomotion by turning in relation to the perceived locations of objects in their visual fields (26). An animal can accomplish this, for example, by turning in a way that moves obstacles away from the center of its visual field, and moves targets toward the center of its visual field (27). Such strategies and their neural mechanisms have primarily been studied in the context of target pursuit (e.g., refs. 26 and 28) or avoidance of stationary obstacles (e.g., ref. 27), but visually guided steering could, in principle, also be used to control evasion trajectories after initiation of an escape maneuver (21).

To determine whether the diverse escape trajectories we observed (Fig. 3 *A* and *B*) could have been generated by a common visual control rule, we computed the visual angle to two key landmarks in the arena—the centroid location of the tablet screen where the stimulus was displayed and the centroid of the coral shelter—for each fish over the course of the maneuver. We hypothesized that fish control their headings, $H(t)$ (degrees), using a control rule with shared deterministic component, $dH(t)/dt = \kappa(t)A(t-\tau) + \mu(t)B(t-\tau)$, where $A(t-\tau)$ is the sine of the angle between the heading vector and the vector pointing to the stimulus (Fig. 3*C*, red arrow), $B(t-\tau)$ is the sine of the angle between the heading vector and the vector pointing to the coral shelter (Fig. 3*C*, blue arrow; sine transformation ensures continuity), and τ is a sensory-motor delay (milliseconds). The coefficients $\kappa(t)$ and $\mu(t)$ (degrees per

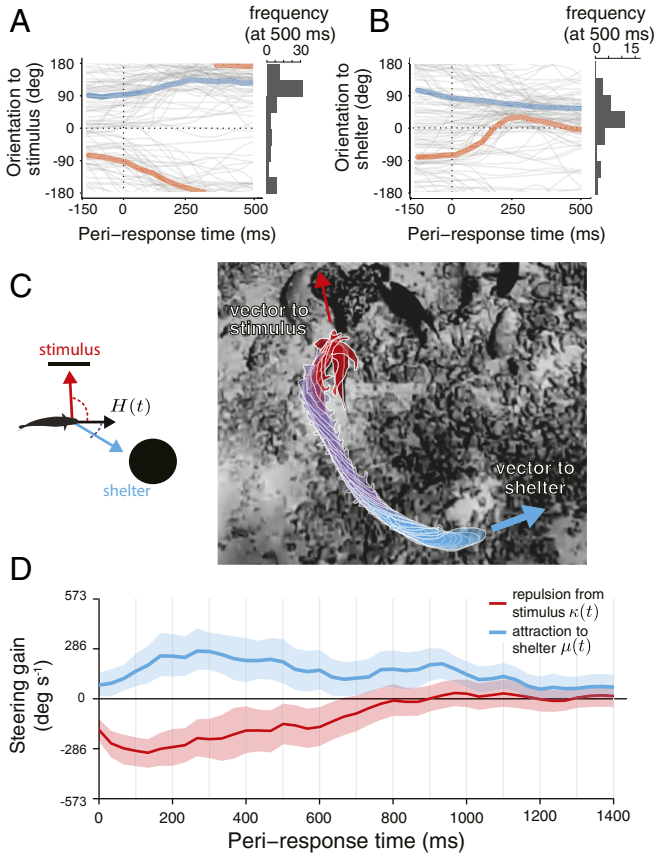

Fig. 3. Fish turn away from threat, then steer toward shelter following a shared time-varying control rule. (*A*) Angle between fish's heading and vector pointing to the stimulus ("orientation to stimulus"). Time 0 marks initiation of escape maneuver. Bold lines show means for fish that began with stimulus in right (orange) or left (blue) visual hemisphere. Vertical histogram shows frequency of tracks falling into each bin at periresponse time = 500 ms. (*B*) Angle between fish's heading and vector pointing to coral shelter. (*C*) Schematic depicting angles to stimulus and shelter (*Left*) and image sequence showing escape maneuver of a parrotfish (*C. sordidus*; *Right*). Colors indicate periods where magnitude of repulsion gain exceeds attraction gain (red), repulsion and attraction gains are similar in magnitude (magenta), and gain term for attraction to shelter exceeds repulsion gain (blue). (*D*) Steering gain terms for repulsion from stimulus [$\kappa(t)$, red line and 90% CI], and attraction toward coral shelter [$\mu(t)$, blue line and 90% CI] over time, computed by fitting DLM to all evasion trajectories of length 500 ms or greater (n = 72 trajectories; *SI Appendix*).

second), which we will refer to as "steering gains," describe whether the fish turns away from (negative coefficient) or toward (positive coefficient) objects. The coefficient magnitude measures the strength of this effect. This control strategy can be thought of as a modified proportional controller with time-varying gain terms, $\kappa(t)$ and $\mu(t)$ (27). We fit this model to evasion trajectories by formulating it as a dynamic linear model (DLM; *SI Appendix*).

The model revealed a progression of turning behavior (Fig. 3*C*) that was shared among diverse escape trajectories (Fig. 3*D*). After initiating an evasion maneuver, fish turned sharply away from the stimulus within the first 200 ms to 300 ms (Fig. 3*D*, red line). They then transitioned to a phase during which steering was dominated by turns that moved the coral shelter toward the center of the visual field (Fig. 3*D*, blue line), aligning direction of travel with the vector pointing to the shelter (Fig. 3*C*). These results are consistent with continuous responses to visual feedback (26, 27), with a shared, time-varying control rule that initially prioritized turns away from the stimulus followed by turns toward shelter. These qualitative patterns were retained when fish were separated by family and the analysis was performed separately for each family (*SI Appendix*, Fig. S5). Similar visual control rules to the one observed here accurately describe obstacle avoidance (27) and target approach (29) behaviors in other species. However, our analysis reveals that, in the case of evasion maneuvers, the gain terms that control turns away from a threat and toward shelter are continually adjusted over the course of the maneuver.

Discussion

Our findings demonstrate how loom-evoked escapes (10, 11) and visually guided steering (26–28) are integrated to generate flexible evasion maneuvers of wild animals. This does not preclude the involvement of sensory modalities other than vision. For example, pressure cues perceived via the lateral line (20) may be involved in avoiding collisions with other individuals. Nevertheless, what initially appears to be substantial variation in response probability (Fig. 2*D*) and escape trajectories (Figs. 1*D* and 3 *A* and *B*) can be captured by a set of conserved decision-making circuits that integrate visual cues to guide decisions about when to flee and how to maneuver out of danger.

A striking feature of responses to looming objects is that they are found across diverse evolutionary lineages (8). This has led to the idea that such responses provide a robust solution to the challenge of evading predators under the varied conditions encountered in nature (7). Our findings support this hypothesis by showing that looming objects reliably trigger escape responses in wild, freely moving animals in a manner consistent with behavioral responses observed in laboratory studies (7) and proposed models of the neural circuits that underlie these responses (8, 10). Future research may help to shed light on the question of why loom responses are so similar across species. For example, signal detection theory (30) may provide a fruitful theoretical framework for determining why the functional form that describes the behavior observed in our study appears to be so widespread.

In addition to supporting the prediction that escape responses involve simultaneous excitation and inhibition by features of an approaching object (1, 7, 24), our results imply that responsiveness may be continuously adjusted based on other features of complex natural scenes, including the locations of nearby individuals. This finding may provide a mechanism for the risk dilution effect exhibited by many animal species (1), a phenomenon that requires that individuals have some means of gauging the density of their neighbors and adjusting escape decisions in response. The neural mechanisms underlying this response plasticity (22, 31) await investigation. However, our findings suggest that information about other individuals may be integrated into decision-making deep within the neural circuits that drive these decisions.

If the kind of conserved decision-making mechanisms revealed here extend to evasion (3, 14) and attack (3, 14, 15) maneuvers of other wild animals, there may be important implications for ecological dynamics, where interactions between predators and prey are often modeled as random outcomes of predator–prey encounters (32). If, as our study suggests, such interactions depend on a limited set of decision-making mechanisms, knowledge of these mechanisms may make it possible to predict outcomes of predator–prey interactions across environmental contexts (33), and to explain the emergence of strong density dependence and feedbacks in consumer resource dynamics (18, 34).

Materials and Methods

Experiments were conducted in the shallow back-reef habitat west of Cook's Pass on the north shore of Mo'orea, French Polynesia (Fig. 1*A*). We

constructed a camera frame from polyvinyl carbonate piping and deployed it in a shallow (~2.5 m depth) reef flat, comprising primarily pavement and coral rubble habitat. This habitat is typical of foraging areas throughout the ecosystem (18). The frame was outfitted with two downward-facing cameras (Hero 3 White; GoPro), allowing us to monitor the area from above. Stimuli were displayed using a tablet computer (iPad Air; Apple Inc.) in a waterproof case, which was mounted vertically to a stand constructed from concrete blocks (Movie S1). Data recorded by the two overhead cameras were combined after projecting all tracks into the field coordinate frame using markers placed at known positions on the base of the camera frame. Camera resolution was 720 by 1,280 pixels.

The looming stimulus was motivated by previous laboratory studies of fish startle responses (10, 11, 22, 35). This stimulus was constructed to simulate an object (a predator) approaching the region in front of the tablet screen using a black ellipse (height = 1.5 × width) that expanded on a white background (Movie S1). When viewed from a distance of 25 cm directly in front of the screen, the looming image corresponded to an object of height 15.3 cm and width 10.2 cm approaching from a starting distance of 6.25 m at a constant speed of 1.78 $m \cdot s^{-1}$ (duration 3.5 s). These parameters are related to the displayed image height $h(t)$, by the equation $h(t) = \hat{h}/(1 + d_0 - vt/d_{screen})$, where $\hat{h}$ is the virtual object true height, v is the virtual approach speed of the object, d_{screen} is the distance between the fish and the screen, and d_0 is the virtual starting distance of the approaching object.

A detailed description of experimental treatments, data processing, and analysis is provided in *SI Appendix*. All experimental procedures were approved by the Princeton University Institutional Animal Care and Use Committee.

ACKNOWLEDGMENTS. We thank B. Martin, S. Munch, and E. Danner for useful comments. This work also benefited from conversations with J. Bak-Coleman. This work was supported by a National Science Foundation (NSF) Postdoctoral Research Fellowship (to M.A.G.) and a McDonnell Foundation Fellowship (to A.M.H.). I.D.C. acknowledges support from NSF Grant IOS-1355061, Office of Naval Research Grants N00014-09-1-1074 and N00014-14-1-0635, Army Research Office Grants W911NG-11-1-0385 and W911NF14-1-0431 (to I.D.C. and S.A.L.), the Struktur-und Innovationsfonds für die Forschung of the State of Baden-Württemberg, and the Max Planck Society. S.A.L. acknowledges Simons Foundation Grant 395890.

1. Cooper WE, Blumstein DT (2015) *Escaping from Predators: An Integrative View of Escape Decisions* (Cambridge Univ Press, Cambridge, UK).
2. Ydenberg RC, Dill LM (1986) The economics of fleeing from predators. *Adv Study Behav* 16:229–249.
3. Wilson AM, et al. (2018) Biomechanics of predator-prey arms race in lion, zebra, cheetah, and impala. *Nature* 554:183–188.
4. Domenici P (2010) Context-dependent variability in the components of fish escape response: Integrating locomotor performance and behavior. *J Exp Zool* 315:59–79.
5. Howland HC (1974) Optimal strategies for predator avoidance: The relative importance of speed and maneuverability. *J Theor Biol* 47:333–350.
6. Scott WL, Leonard NE (2018) Optimal evasive strategies for multiple interacting agents with motion constraints. *Automatica* 94:26–34.
7. Fotowat H, Gabbiani F (2011) Collision detection as a model for sensory-motor integration. *Annu Rev Neurosci* 34:1–19.
8. Peek MY, Card GM (2016) Comparative approaches to escape. *Curr Opin Neurobiol* 41:167–173.
9. Klapoetke NC, et al. (2017) Ultra-selective looming detection from radial motion opponency. *Nature* 551:237–241.
10. Dunn TW, et al. (2015) Neural circuits underlying visually evoked escapes in larval zebrafish. *Neuron* 25:1823–1834.
11. Temizer I, Donovan JC, Baier H, Semmelhack JL (2015) A visual pathway for looming-evoked escape in larval zebrafish. *Curr Biol* 25:1823–1834.
12. Rosenthal SB, Twomey CR, Hartnett AT, Wu HS, Couzin ID (2015) Revealing the hidden networks of interaction in mobile animal groups allows prediction of complex behavioral contagion. *Proc Natl Acad Sci USA* 112:4690–4695.
13. Stankowich T, Blumstein DT (2005) Fear in animals: A meta-analysis and review of risk assessment. *Proc R Soc B* 272:2627–2634.
14. Amador Kane SA, Fulton AJ, Rosenthal LJ (2015) When hawks attack: Animal-borne video studies of goshawk pursuit and prey-evasion strategies. *J Exp Biol* 218:212–222.
15. Brighton CH, Thomas ALR, Taylor GK (2017) Terminal attack trajectories of peregrine falcons are described by the proportional navigation guidance law of missiles. *Proc Natl Acad Sci USA* 114:13495–13500.
16. Gil MA, Zill J, Ponciano JM (2017) Context-dependent landscape of fear: Algal density elicits risky herbivory in a coral reef. *Ecology* 98:534–544.
17. White JW, et al. (2010) Synthesizing mechanisms of density dependence in reef fishes: Behavior, habitat configuration, and observational scale. *Ecology* 91:1949–1961.
18. Gil MA, Hein AM (2017) Social interactions among grazing reef fish drive material flux in a coral reef ecosystem. *Proc Natl Acad Sci USA* 114:4703–4708.
19. Januchowski-Hartley FA, Graham NA, Feary DA, Morove T, Cinner JE (2011) Fear of fishers: Human predation explains behavioral changes in coral reef fishes. *PLoS One* 6:e22761.
20. Oteiza P, Odstrcil I, Lauder G, Portuges R, Engert F (2017) A novel mechanism for mechanosensory-based rheotaxis in larval zebrafish. *Nature* 547:445–448.
21. Eaton RC, Emberley DS (1991) How stimulus direction determines the trajectory of the mauthner-initiated escape response in a teleost fish. *J Exp Biol* 161:469–487.
22. Bhattacharyya K, McLean DL, MacIver MA (2017) Visual threat assessment and reticulospinal encoding of calibrated responses in larval zebrafish. *Curr Biol* 27:2751–2762.
23. Silva AC, McMillan GA, Santos CP, Gray JR (2015) Background complexity affects response of a looming-sensitive neuron to object motion. *J Neurophysiol* 113:218–231.
24. Hatsopoulos N, Gabbiani F, Laurent G (1995) Elementary computation of object approach by a wide-field visual neuron. *Science* 270:1000–1003.
25. Marshall NJ, Jennings K, McFarland WN, Loew ER, Losey GS (2013) Visual biology of Hawaiian coral reef fishes. III. Environmental light and an integrated approach to the ecology of reef fish vision. *Copeia* 3:467–480.
26. Poggio T, Reichardt W (1973) A theory of the pattern induced flight orientation of the fly *Musca domestica*. *Kybernetik* 12:185–203.
27. Lin H, Ros IG, Biewener AA (2014) Through the eyes of a bird: Modeling visually guided obstacle flight. *J R Soc Interface* 11:20140239.
28. Gahtan E, Tanger P, Baier H (2005) Visual prey capture in larval zebrafish is controlled by identified reticulospinal neurons downstream of the tectum. *J Neurosci* 25:9294–9303.
29. Land MF, Collett TS (1974) Chasing behaviour of houseflies (*Fannia canicularis*). *J Comp Physiol* 89:331–357.
30. Green DM, Swets JA (1966) *Signal Detection Theory and Psychophysics* (Wiley, New York).
31. Salay LD, Ishiko N, Huberman AD (2018) A midline thalamic circuit determines reactions to visual threat. *Nature* 557:183–189.
32. Gurarie E, Ovaskainen O (2012) Towards a general formalization of encounter rates in ecology. *Theor Ecol* 6:189–202.
33. Pawar S, Dell AI, Savage VM (2012) Dimensionality of consumer search space drives trophic interaction strengths. *Nature* 486:485–489.
34. Courchamp F, Clutton-Brock T, Grenfell B (1999) Inverse density dependence and the allee effect. *Trends Ecol Evol* 14:405–410.
35. Preuss T, Osei-Bonsu PE, Weiss SA, Wang C, Faber DS (2006) Neural representation of object approach in a decision-making motor circuit. *J Neurosci* 26:3454–3464.